

Effect of Electrochemical Oxidation-Reduction Cycles on Surface Structures and Electrocatalytic Oxygen Reduction Activity of Au Electrodes

Taejung Lim and Jongwon Kim*

Department of Chemistry, Chungbuk National University, Cheongju 28644, Korea.

**E-mail: jongwonkim@chungbuk.ac.kr*

(Received June 22, 2016; Accepted August 4, 2016)

ABSTRACT. Oxidation-reduction cycling (ORC) procedures are widely used for cleaning nanoparticle surfaces when investigating their electrocatalytic activities. In this work, the effect of ORC on the surface structures and electrocatalytic oxygen reduction activity of Au electrodes is analyzed. Different structural changes and variations in electrocatalysis are observed depending on the initial structure of the Au electrodes, such as flat bulk, nanoporous, nanoplate, or dendritic Au. In particular, dendritic Au structures lost their sharp-edge morphology during the ORC process, resulting in a significant decrease in its electrocatalytic oxygen reduction activity. The results shown in this paper provide an insight into the pretreatment of nanoparticle-based electrodes during investigation of their electrocatalytic activities.

Key words: Oxidation-reduction cycle, Surface structure, Oxygen reduction, Electrocatalyst

INTRODUCTION

Metal nanoparticles, due to their unique characteristics, have properties that are different from those of the bulk metal, and are consequently being utilized in various fields.¹ Recently, several synthesis methods for controlling the size and shape of metal nanoparticles have been developed. The electrocatalytic activity of such controlled metal nanoparticles has also been investigated, and their development as highly efficient catalysts has been actively pursued.^{2,3} Especially, the influence of the shape and size of metal nanoparticles on their catalytic activity for the electrochemical oxygen reduction reaction, which plays an important role in the development of the cathode of fuel cells, has been studied by numerous researchers.^{4,5}

Generally, in order to prevent the coagulation of nanoparticles during their synthesis, and to control the shape of the nanoparticle, a stabilizing agent or an additive is used. However, such organic molecules, which surround the nanoparticle, are likely to decrease the electrocatalytic activity of the nanoparticle.⁶ Therefore, to observe the unique electrocatalytic activity of the metal nanoparticle, the organic molecules including the stabilizing agent or additive, which surround the nanoparticle should be removed after depositing the metal nanoparticle on the electrode surface. To obtain a clean metal electrode surface, a suggestive general method is to repetitively cycle the potential in acidic condition, thereby removing the organic material from the surface of the nanoparticles constituting the electrode.⁶ As the metal sur-

face is oxidized and reduced continuously, debris such as organic materials present on the surface of the metal are removed, so that a clean metal nanoparticle surface can be obtained.

Although the repetitive electrochemical oxidation-reduction cycling (ORC) process is effective for cleaning the surface of a metal, the unique shape of the metal nanoparticle can also change.^{7,8} Based on previously reported studies, a predetermined amount of the metal gets dissolved during oxidation of the metal surface.⁹⁻¹¹ Therefore, a study confirming the possibility of structural changes of the metal nanoparticle, which can occur during the electrochemical cleaning of the metal surface, is expected to be of tremendous importance for understanding the electrocatalytic activity of the metal nanoparticle.

In the present study, changes to the metal surface when applying electrochemical ORC on gold (Au) surface, and the influence of these modifications on the catalytic activity for the electrochemical oxygen reduction were examined. The changing modes of the surface and oxygen reduction activity by ORC were tested, compared, and analyzed in flat bulk, nanoporous, nanoplate, and dendrite gold electrodes.

EXPERIMENT

All the solutions were prepared in purified water (Milli-Q, 18.2 M Ω ·cm), and 0.1 M sulfuric acid solution was chosen as the electrolyte. Sulfuric acid and ethanol were purchased from Merck, Techni Gold 25 ES, Technic Inc.,

$\text{KAu}(\text{CN})_2$ was acquired from Alfa Aesar, and other reagents were procured from Aldrich. CHI 600E (CHI Instrument) was used to perform the electrochemical experiments. Pt wire and Ag/AgCl electrode (3 M NaCl) were, respectively, employed as the auxiliary and reference electrode. The surface of the flat gold electrode was examined via the Dimension ICON atomic force microscope (AFM), Bruker. The surface morphology of the nanostructured gold electrode was analyzed by using the ULTRA PLUS scanning electron microscope (SEM) of Carl Zeiss.

The flat gold electrode was tested using a gold rod electrode (CHI Instrument, inner diameter: 2.0 mm). Electrochemical measurements were performed with the gold rod electrode after polishing it for 5 min, in the order of decreasing particle size (from 5.0 μm to 0.05 μm) by using a diamond suspension (Buehler). The nanoporous gold electrode was manufactured by the method reported in previous studies,¹² which involves 25 s of anodizing. The nanoplate and dendrite gold electrodes, wherein the gold substrate electrodes are vacuum-deposited on silicon wafers, were washed and used as working electrodes, while the surface was limited by an O-ring (Viton) with an inner diameter of 2.9 mm. The nanoplate gold electrode was prepared by the method reported in an earlier work, which applies a potential of -1.1 V to 15 mM $\text{KAu}(\text{CN})_2$ and 0.25 M Na_2CO_3 solution mixture.¹³ The dendrite nanostructure was generated by applying -0.85 V from the sulfite-based gold solution (Techni Gold 25 ES), as described in a precedent study.¹⁴

RESULTS AND DISCUSSION

Fig. 1 shows the cyclic voltammograms during 40 ORC cycles conducted on the flat gold electrode. Starting from an electrode potential of 0.5 V, the scanning was first carried out in the negative direction. After confirming the reduction peak (peak I), which corresponds to the electrochemical oxygen reduction activity of the initial gold electrode surface, the direction of electrode potential was reversed to the positive direction, in order to oxidize the gold surface (peak II). After that, the potential was again shifted to the negative direction, in order to reduce the surface (peak III) and the procedure was repeated. In the continuous ORC process, the current of peaks II/III, corresponding to the oxidation and reduction of the gold surface, increased systematically. The magnitude of the oxidation-reduction current of gold surface reflects the electrochemical surface area (ESA).¹⁵ Therefore, the above results indicate that ESA of the flat gold electrode gradually increases through repetitive ORC process. Simultaneously, during the repeating

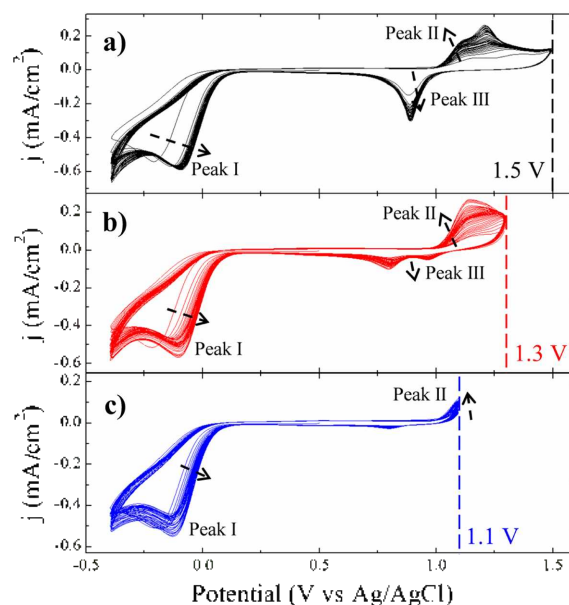


Figure 1. Cyclic voltammetry of 40 ORC cycles, conducted on the flat gold electrode by adjusting the upper potential limit (E_U), under oxygen-saturated 0.1 M sulfuric acid (Scan Rate = 50 mV/s). (a) $E_U = 1.5$ V, (b) $E_U = 1.3$ V, and (c) $E_U = 1.1$ V.

ORC, the peak potential of the electrochemical oxygen reduction shifts towards the positive direction. This is suggestive of an improvement in the oxygen reduction activity of the gold surface.

The degree of gold surface oxidation can be adjusted by the upper potential limit (E_U) of the oxidation process. The differences in the oxidation degrees during the ORC process are compared in Fig. 1. At $E_U = 1.5$ V oxidation of the gold surface is complete, and a rapid increase in oxygen reduction occurs during the two initial ORC processes. Thereafter, the enhancement becomes gradual. When E_U decreases to 1.3 V during the oxidation of the gold surface, the increase of oxygen reduction catalytic activity during ORC becomes slow compared to $E_U = 1.5$ V condition. At $E_U = 1.1$ V, the rate of oxygen reduction activation becomes even slower. The above results indicate that, when the degree of oxidation-reduction of the gold surface becomes greater, the changes of the surface become more rapid, thus resulting in swifter enhancement of oxygen reduction catalytic activity.

Fig. 2a compares the oxygen reduction catalytic activity that is obtained after the continuous ORC process on the flat gold electrode with the activity prior to ORC. The peak potential of the initial oxygen reduction activity of the flat gold surface, which underwent physical polishing, was

observed at -0.21 V. After the repetition of ORC process at $E_U = 1.5$ V, the catalytic activity was enhanced, and the peak potential shifted to -0.09 V. When E_U of the ORC process was decreased to 1.3 and 1.1 V, the oxygen reduction peak potentials were observed at -0.11 and -0.13 V, respectively. The results suggest that, as the degree of the oxidation and reduction of the gold surface increases, the enhancement of the oxygen reduction catalytic activity after the ORC process increases. At the end of ORC process, along with the change in the peak potential of the oxygen reduction reaction, an increase in the peak current is also observed. This is due to the increase of ESA, which occurs during the ORC as observed in Fig. 1.

In order to confirm the changes to the flat gold surface induced by the ORC process, the AFM images of the flat gold electrode before (Fig. 2b) and after (Fig. 2c) ORC were obtained and compared. The AFM image of the flat gold electrode, which underwent physical polishing, is shown in Fig. 2b. Although, there are some curves on the gold surface, these are in general smooth. Further, some flaws are generated by the polishing particles used during the physical polishing. The AFM image of the flat gold electrode obtained after the ORC process is shown in Fig. 2c. The figure illustrates that the surface roughness was increased by the ORC process. The root mean square roughness (RMS) before ORC (19.6) increased to 42.3 after the ORC process. The changes in the roughness induced by the ORC process well describe the increase in both the surface area, which is electrochemically measured, and the peak current of the oxygen reduction reaction. It was confirmed from the AFM images that the gold electrode surface, which comprised of a smooth curved surface prior to the ORC process, showed angular faces after the ORC process. Generally, an angular and sharp metal surface is known to have higher oxygen reduction catalytic activity than a smooth and curved metal surface.^{16,17} Therefore, the shift of the electrochemical oxygen reduction peak potential towards the positive direction in the flat gold surface after the ORC process can be understood as an enhancement of its catalytic activity due to the changes in the surface shape.

Fig. 3 displays the cyclic voltammograms obtained from the repetitive ORC process on the nanoporous gold electrode. As ORC proceeds initially on the nanoporous gold electrode formed by anodization, the peaks of oxidation (peak II) and reduction (peak III) of the gold surface decreased systematically. This result is in contrast to that shown by the flat gold electrode (see Fig. 1). In case of the nanoporous gold electrode, as the ORC process repeats, ESA decreases. The peak potential, which corresponds to the electrochemical

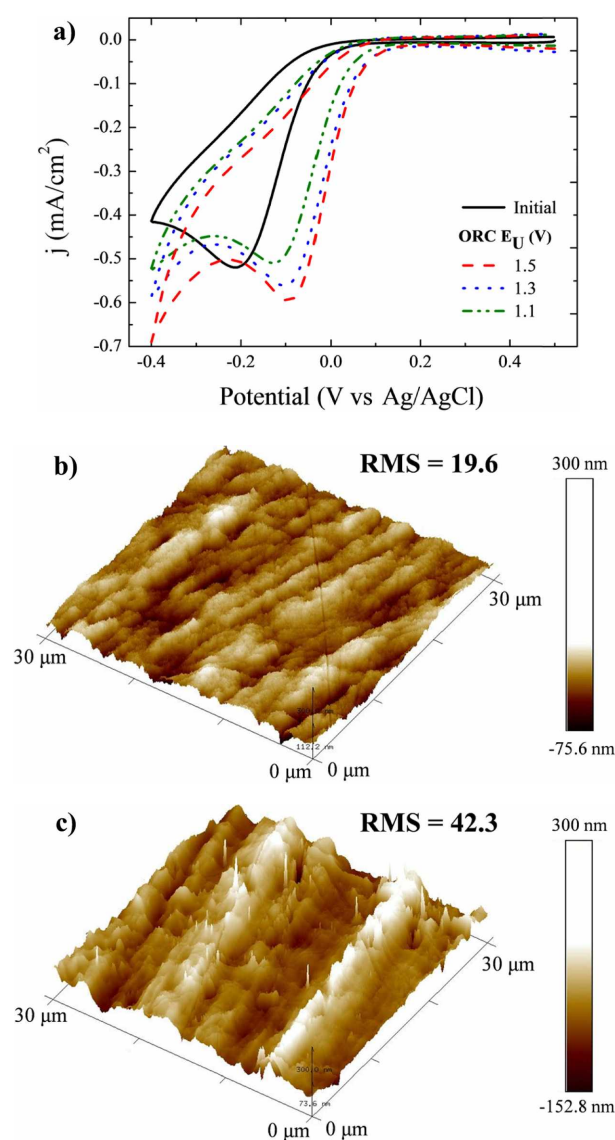


Figure 2. (a) Cyclic voltammetry, comparing the initial oxygen reduction on the flat gold electrode with the last oxygen reduction derived after the 40 ORC cycles that were conducted at different E_U in Fig. 1 (Scan Rate = 50 mV/s). AFM image of the flat gold electrode (b) immediately after physical polishing (30 μ m \times 30 μ m) and (c) after undergoing 40 ORC cycles at $E_U = 1.5$ V (30 μ m \times 30 μ m).

oxygen reduction of the nanoporous gold surface, shifted slightly towards the negative direction, as the ORC process proceeded. Therefore, the nanoporous gold electrode is predicted to show an insignificant increase or even a decrease in the oxygen reduction catalytic activity. This result is also opposite to that for the flat gold electrode. Overall, variation of E_U during the ORC process did not significantly influence the trend of catalytic activity.

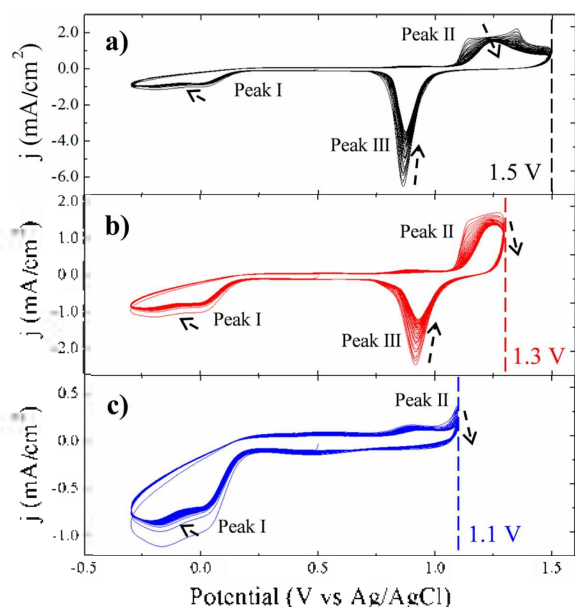


Figure 3. Cyclic voltammetry of 40 ORC cycles conducted on the nanoporous gold electrode while adjusting E_U under oxygen-saturated 0.1 M sulfuric acid (Scan Rate = 50 mV/s). (a) $E_U = 1.5$ V, (b) $E_U = 1.3$ V, and (c) $E_U = 1.1$ V.

Fig. 4a compares the oxygen reduction catalytic activity of the nanoporous gold electrode before and after the continuous ORC process. The peak potential of the initial oxygen reduction activity of the nanoporous gold electrode formed by the anodization was measured at 0.01 V. This is an even greater enhancement of the maximum oxygen reduction activity than that obtained by repeating the ORC process on the flat gold electrode (peak potential of -0.09 V). Therefore, the nanoporous gold surface shows better catalytic activity than the flat gold surface, due to its nanostructured surface. On the nanoporous gold surface, unlike the flat gold electrode, one more reduction peak is observed at approximately -0.17 V during the oxygen reduction. This refers to an additional reduction of hydrogen peroxide, which was generated by the oxygen reduction, into water, and is a commonly observed phenomenon on a nanostructured gold surface.¹⁸

Figs. 4b and 4c compare the SEM images of the surface structures of nanoporous gold before and after the ORC process. On the surface of nanoporous gold generated by anodization (Fig. 4b) ligament and pore structures of 50 nm width are found to be well developed. After undergoing the repetitive ORC process (Fig. 4c), the width of the ligament structure increased to ~ 100 nm. It is believed that expansion of the ligament structure occurs as gold oxide is

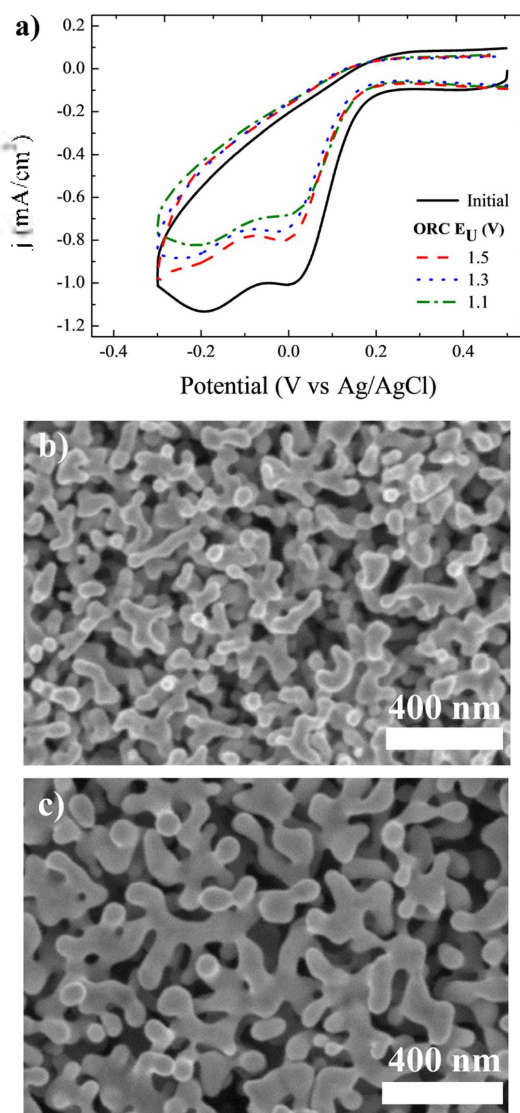


Figure 4. (a) Cyclic voltammetry comparing the initial oxygen reduction on the nanoporous gold electrode with the last oxygen reduction derived after 40 ORC cycles performed at different E_U in Fig. 3 (Scan Rate = 50 mV/s). SEM image of the nanoporous gold electrode (b) immediately after anodization and (c) after undergoing 40 ORC cycles at $E_U = 1.5$ V.

formed, which is then again reduced to gold on the surface of the nanoporous structure during the ORC process. The expansion of the ligament structure during ORC explains the decrease of ESA as shown in Fig. 3. However, even after undergoing the ORC process, the nanostructured curved gold surface was not significantly affected. Therefore, it can be inferred that no substantial changes in the electrochemical oxygen reduction activity occur.

Fig. 5a compares the initial oxygen reduction activity of

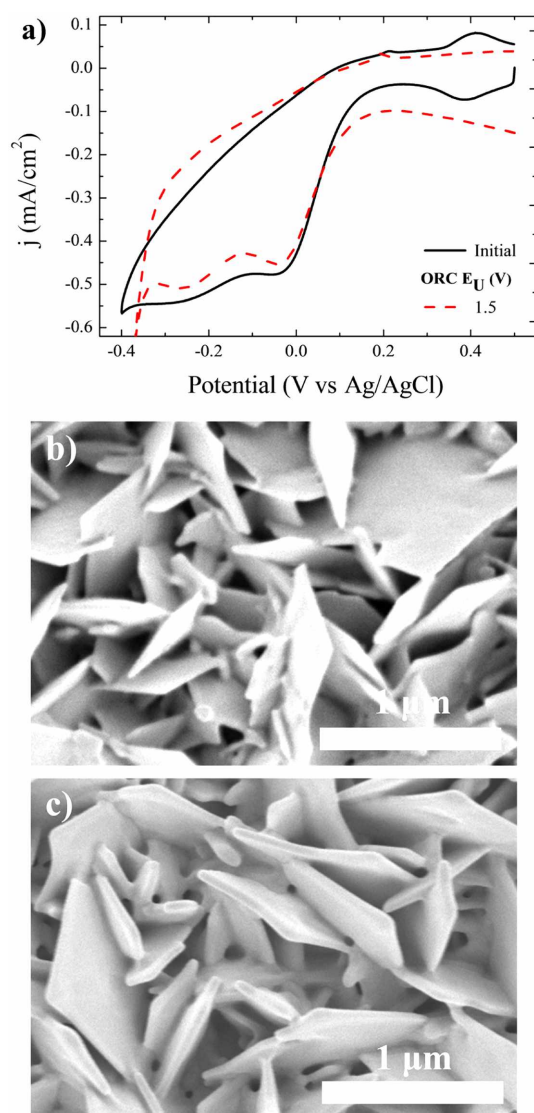


Figure 5. (a) Cyclic voltammetry comparing the initial oxygen reduction on the nanopl原因 gold electrode with the last oxygen reduction derived after 40 ORC cycles at different E_U (Scan Rate = 50 mV/s). SEM image of nanopl原因 gold electrode (b) immediately after the formation and (c) after undergoing 40 ORC cycles at $E_U = 1.5$ V.

the nanopl原因 gold electrode, formed by electrochemical deposition, with the oxygen reduction activity after the ORC process. The peak potential of the initial oxygen reduction of nanopl原因 gold electrode was measured at around 0.0 V. This catalytic activity is better than that of the flat gold electrode, but not as good as that of the nanoporous gold electrode. Fig. 5b shows the SEM image of the nanopl原因 gold surface immediately after electrochemical deposition. The maximum width of the nanopl原因 surface on average is about 800 nm. Although corners are present in the nano-

plate, it is mostly composed of flat gold surfaces, so that the catalytic activity is mediocre. Even after the ORC process, the oxygen reduction catalytic activity on the surface of the nanopl原因 was found to be similar to the activity prior to the ORC process. The surface shape of the nanopl原因 after the ORC process (Fig. 5c) also did not show significant differences compared to the surface shape before the ORC process. Although the corners of the nanopl原因 gold rounded out slightly, such structural changes derived from the ORC process do not significantly influence the oxygen reduction catalytic activity.

Summing up the results in so far, the surface of flat bulk gold exhibits an enhancement of oxygen reduction catalytic activity by acquiring a rougher surface and active sites during the ORC process. On the other hand, the nanoporous gold with round surface and nanopl原因 gold with smooth surface showed almost no change in the oxygen reduction catalytic activity even after undergoing the ORC process. Finally, the electrochemical changes of the dendrite gold structures, with spiky nanostructure tens of nanometer in size, observed during the ORC process are shown in Fig. 6. When the ORC process progresses on the dendrite gold electrode, the peak current of the oxidation (peak II) and reduction (peak III) of the dendrite gold surface decreased more rapidly than of the other types of gold surface studied herein. This

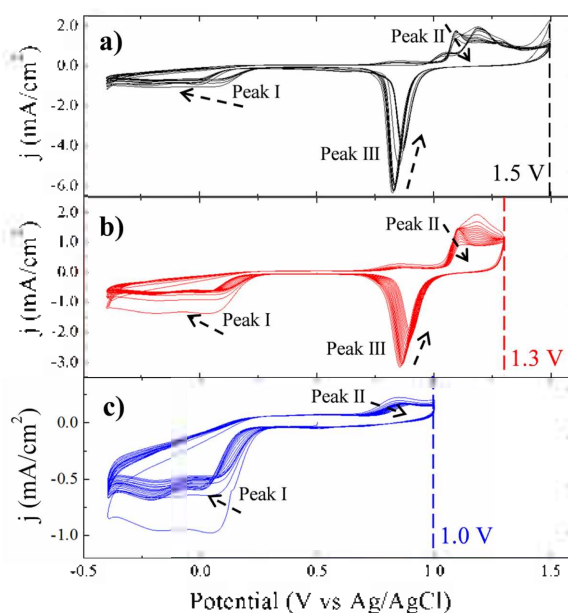


Figure 6. Cyclic voltammetry of ORC conducted on the dendrite gold electrode by adjusting E_U and cycle number under oxygen-saturated 0.1 M sulfuric acid (Scan Rate = 50 mV/s). (a) 14 Cycles at $E_U = 1.5$ V, (b) 18 Cycles at $E_U = 1.3$ V, and (c) 20 Cycles at $E_U = 1.1$ V.

indicates that the structural changes made to the dendrite gold surface are significant on undergoing the ORC process. Therefore, for the dendrite gold electrode the number of repetitive ORC processes was reduced until no change of oxygen reduction catalytic activity was observed. The peak potential, which refers to the electrochemical oxygen reduction on the dendrite gold surface, drastically shifted towards the negative direction due to the ORC process. As the upper potential limit of the ORC process shifted towards the negative direction, the magnitude of catalytic activity change decreased.

Fig. 7a compares the initial oxygen reduction activity of the dendrite gold electrode with the activity after the ORC process. The initial oxygen reduction peak of the dendrite gold electrode formed by the electrochemical deposition was observed at 0.08 V. This indicates that the oxygen reduction catalytic activity of the dendrite gold surface is better than that of the nanoporous and nanoplate gold electrodes. Under the condition of E_U of 1.5 V, the ORC process was repeated 14 times. After that, the oxygen reduction catalytic activity decreased and the peak current was measured at around 0.0 V. When E_U of ORC process was decreased, the change in magnitude of catalytic activity decreased and the number of cycles it took for the decrease of oxygen reduction catalytic activity to stop increased. This is opposite to the results obtained for nanoporous and nanoplate gold electrodes, for which the ORC process did not significantly influence the catalytic activity.

To confirm the changes to the dendrite gold structure induced by the ORC process, the SEM images obtained before and after ORC are shown in Figs. 7b and 7c, respectively. It can be seen from Fig. 7b that the dendrite gold structure obtained after electrochemical deposition possesses well-developed sharp bumps of sizes less than 30 nm. These structural features are evidently the reason for its catalytic activity being greater than the other nanostructured gold electrodes investigated in this study. However, after the ORC process, the sharp bumps on the dendrite gold structure disappear, and only a round-surfaced gold pillar remains (Fig. 7c). Furthermore, the dendrite gold structures of relatively smaller sizes are no longer present. When gold oxide is formed on the surface, and is reconverted to gold upon reduction during the ORC process, bumps with relatively high surface energy and small dendrite structures are deformed. Due to such changes to the surface, the oxygen reduction catalytic activity is greatly reduced after the ORC process and decrease in reduction current occurs, due to the decrease of ESA on the gold surface. Therefore, unlike nanoporous gold with a round surface and nanoplate gold with a smooth

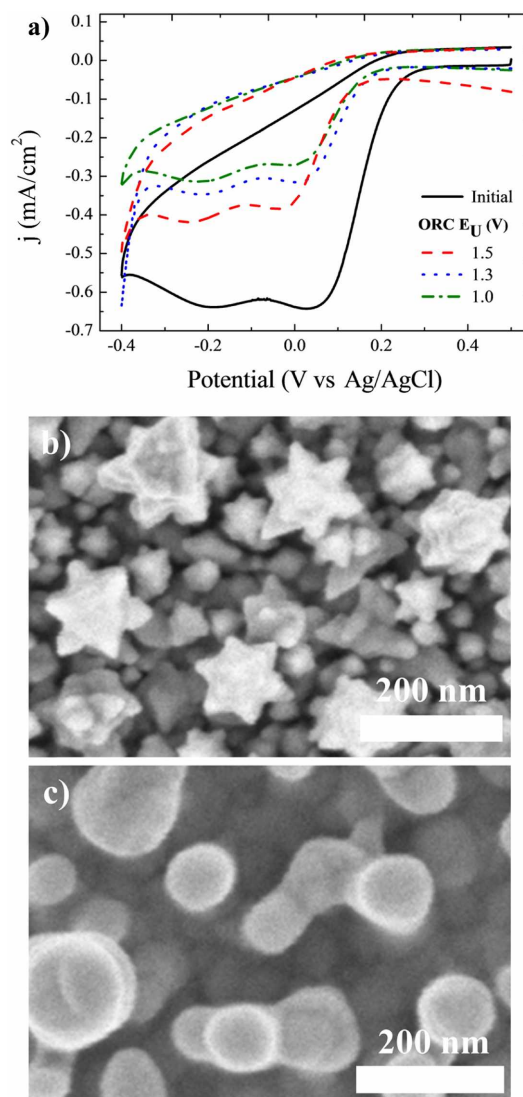


Figure 7. (a) Cyclic voltammetry comparing the initial oxygen reduction on the dendrite gold electrode with the last oxygen reduction derived from ORC conducted at different E_U and number of cycles (Scan Rate = 50 mV/s). SEM image of the dendrite gold electrode surface (b) immediately after formation and (c) after undergoing 14 ORC cycles at $E_U = 1.5$ V.

surface, the surface of dendrite gold, which possesses sharp features, greatly changes during the ORC process. Therefore, the ORC results in loss of oxygen reduction catalytic activity of the unique initial gold nanostructure.

CONCLUSIONS

In the present study, the influence of the electrochemical ORC process, which is utilized for cleaning nanostructured electrode surfaces, on the surface structure of the gold

electrode, and thereby changes in the oxygen reduction catalytic activity were investigated. To examine the effect on the initial shape of the gold electrode, flat bulk, nanoporous, nanoplate, and dendrite gold electrodes were subjected to the ORC process. In the case of flat bulk gold, the surface roughness increased and the oxygen reduction catalytic activity was enhanced through the ORC process. The nanoporous gold with round surface and nanoplate gold with smooth surface did not undergo drastic changes in their surface structures after completion of the ORC process, thus resulting in no significant increase in their oxygen reduction catalytic activities. The dendrite gold surface, with the spiky nanostructure of the order of a few nanometers in size, was devoid of the spiky bumps after ORC, so that the oxygen reduction catalytic activity decreased. The above results confirmed that depending on the initial form of the gold surface, the changes induced by the ORC process to the surface can differ, and consequently, the effect on the oxygen reduction catalytic activity can vary. The results of the present study are important concerning the precautions that must be taken during pre-treatment of electrodes in electrochemical experiments when investigating the electrocatalytic activity of nanostructures.

Acknowledgments. This work was supported by the National Research Foundation of Korea (NRF) grant funded by the Korea government (MSIP) (No. 2014R1A2A1A11050622).

REFERENCES

1. Daniel, M. C.; Astruc, D. *Chem. Rev.* **2004**, *104*, 293.
2. Bandarenka, A. S.; Koper, M. T. M. *J. Catal.* **2013**, *308*, 11.
3. Solla-Gullon, J.; Vidal-Iglesias, F. J.; Feliu, J. M. *Annu. Rep. Prog. Chem., Sect. C: Phys. Chem.* **2011**, *107*, 263.
4. Gewirth, A. A.; Thorum, M. S. *Inorg. Chem.* **2010**, *49*, 3557.
5. Stephens, I. E. L.; Bondarenko, A. S.; Gronbjerg, U.; Rossmeisl, J.; Chorkendorff, I. *Energy Environ. Sci.* **2012**, *5*, 6744.
6. Kleijn, S. E. F.; Lai, S. C. S.; Koper, M. T. M.; Unwin, P. R. *Angew. Chem. Int. Ed.* **2014**, *53*, 3558.
7. K ntje, C.; Kolb, D. M.; Jerkiewicz, G. *Langmuir* **2013**, *29*, 10272.
8. Lim, B.; Jiang, M. J.; Camargo, P. H. C.; Cho, E. C.; Tao, J.; Lu, X. M.; Zhu, Y. M.; Xia, Y. A. *Science* **2009**, *324*, 1302.
9. Cherevko, S.; Topalov, A. A.; Katsounaros, I.; Mayrhofer, K. J. J. *Electrochem. Commun.* **2013**, *28*, 44.
10. Lee, S. B.; Kwon, J.; Kim, J. *Electroanalysis* **2015**, *27*, 2180.
11. Zu, Y.; Bard, A. J. *Anal. Chem.* **2000**, *72*, 3223.
12. Kim, M.; Kim, J. *Langmuir* **2014**, *30*, 4844.
13. Seo, B.; Choi, S.; Kim, J. *ACS Appl. Mater. Interfaces* **2011**, *3*, 441.
14. Ahn, M.; Kim, J. *J. Electroanal. Chem.* **2012**, *683*, 75.
15. Trasatti, S.; Petrii, O. A. *Pure Appl. Chem.* **1991**, *63*, 711.
16. Erikson, H.; Sarapuu, A.; Alexeyeva, N.; Tammeveski, K.; Solla-Gull n, J.; Feliu, J. M. *Electrochim. Acta* **2012**, *59*, 329.
17. Yu, T.; Kim, D. Y.; Zhang, H.; Xia, Y. *Angew. Chem. Int. Ed.* **2011**, *50*, 2773.
18. El-Deab, M. S.; Ohsaka, T. *Electrochem. Commun.* **2002**, *4*, 288.